Very Black Infrared Detector from Vertically Aligned Carbon Nanotubes and Electric-Field Poling of Lithium Tantalate

John Lehman,* and Aric Sanders

Optoelectronics Division, National Institute of Standards and Technology, Boulder, Colorado 80305

Leonard Hanssen, Boris Wilthan, and Jinan Zeng

Optical Technology Division, National Institute of Standards and Technology, Gaithersburg, Maryland, 20899

Christopher Jensen

Materials Science and Engineering, Stony Brook University, Stony Brook, New York 11794

ABSTRACT Vertically aligned multiwall carbon nanotubes were grown by water-assisted chemical vapor deposition on a large-area lithium tantalate pyroelectric detector. The processing parameters are nominally identical to those by which others have achieved the "world's darkest substance" on a silicon substrate. The pyroelectric detector material, though a good candidate for such a coating, presents additional challenges and outcomes. After coating, a cycle of heating, electric field poling, and cooling was employed to restore the spontaneous polarization perpendicular to the detector electrodes. The detector responsivity is reported along with imaging as well as visible and infrared reflectance measurements of the detector and a silicon witness sample. We find that the detector responsivity is slightly compromised by the heat of processing and the coating properties are substrate dependent. However, it is possible to achieve nearly ideal values of detector reflectance uniformly less than 0.1 % from 400 nm to 4 μm and less than 1 % from 4 to 14 μm.

KEYWORDS Absorptance, carbon nanotube, optical coating, pyroelectric detector, reflectance, spectral responsivity, thermal detector.

Since the 19th century the world has sought a better thermal detector for radiometry.[1] When we think of making a better thermal detector we consider improving the intrinsic properties of the detector element, such as the pyroelectric coefficient (of a pyroelectric detector) or the temperature coefficient of resistance (for a bolometer). To increase the efficiency of converting photons to heat, we also want to make the detector as black as possible with the addition of a coating. Since thermal detectors are capable of operating over a broad wavelength range, we prefer the black coating to have 100 % absorption efficiency over a large part of the visible and infrared spectrum (400 nm to 50 μm). At NIST and elsewhere, the basis of standards for measuring optical radiance, irradiance, and the definition of the candela are based on a thermal detector of one sort or another. In nearly every case, these detectors have a black coating to enhance detection efficiency and spectral uniformity. Thus, our ability to make better coatings supports our ability to make more accurate measurements for a variety of NIST priorities such as optical fiber-based communication systems, photovoltaic and solar-thermal efficiency, satellite-based sensors for earth and sun temperature measurements, and laser-based manufacturing.

We seek to optimize thermal properties, reproducible topology, and fabrication. In addition to scientific interest, our goal is to make practical use of the optimal coating material by applying it to a thermal detector. Very black coatings typically have a percolated structure.[2] Structures such as nanofractal gold (gold black) and nickel phosphorus and various carbon-based coatings have been reported having reflectance as low as 1 % over a broad wavelength range, but the thermal conductivity is at least ten times lower than that published for carbon nanotubes (carbon nanotubes being in the range of 300 to 3000 W/mK).[3,4] As we achieve a structure that is sparse enough to absorb longer wavelengths efficiently, the thermal conductivity becomes less efficient due to the fewer points of material contact and thus reduced phonon transport. The highest thermal conductivity and lowest specific heat is desirable. In 1933, the first nanofractal gold (gold black) coatings were reported and remain among the blackest absorbers that we can make for a broad wavelength range. In the past, we have reported black coatings such as gold black and single wall carbon

nanotubes.[5,6] We have also investigated random mats of multiwalled carbon nanotubes (MWCNTs) and vertically aligned multiwall carbon nanotubes (VAMWCNTs) on a LiNbO$_3$ pyroelectric detector.[7,8] We have investigated optical properties and laser damage mechanisms of CNTs on pyroelectric detectors and a flowing-water power meter.[9] Itkis et al. investigated a random mat of SWCNTs to form a bolometric detector.[10] Recently, several authors have reported coatings that have desirable properties for our application. For example, in this journal, Yang et al. described VAMWCNTs that were considered the world's "darkest material".[11] More recently, Mizuno et al. attained extremely low reflectance (uniformly less than 0.01) at wavelengths from the visible to 200 μm.[12] The "world's darkest detector" is a logical progression and a very practical application of nanotechnology. We have overcome challenges while trying to reproduce previous work by optimizing the requirements of a desirable coating and physical properties of the detector.

The pyroelectric detector consists of a disk of z-cut lithium tantalate (LiTaO$_3$) 12 mm in diameter and 60 μm thick. Metal electrodes 10 mm in diameter were deposited on each face of the crystal, 25 nm of chromium followed by 50 nm of gold on the front side and 25 nm of chromium on the back. Additional details of this type of pyroelectric detector are found elsewhere.[6] The area of VAMWCNTs grew from a 2 nm thick iron catalyst on top of a 20 nm buffer layer of aluminum. The detector area was masked such that the aluminum and iron were deposited onto an 8 mm diameter area, underfilling the gold electrode.

A vertically aligned MWCNT forest was grown by First-Nano, a division of CVD Equipment Corporation, using a water-assisted chemical vapor deposition (CVD) process similar to that previously reported by Ci et al.[13] Briefly, the process consists of a 2.5 min growth at 750 °C whereby 100 standard cubic centimeters per minute (sccm) ethylene, 195 sccm hydrogen, 1.1 standard liters per minute (slpm) argon, and 40 sccm argon passed through a water bubbler and injected into the reactor at room temperature. Upon completion of the growth, the system was cooled to room temperature in a mixture of argon and hydrogen gas. To repole the crystals, they were placed in a gap between two plates capable of producing a high-voltage DC electric field. The detector was heated to 750 °C and soaked for 10 min in argon. The furnace was then turned off and the DC field was turned on. As the crystal passed through the Curie temperature (~665 °C), a DC field of 230 V/mm was present.

The detector evaluation was accomplished by a combination of methods: (1) near-normal hemispherical reflectance with a Fourier Transform Infrared (FTIR) spectrometer from 1 to 14 μm;[14,15] (2) absolute spectral responsivity with a blackbody source and a continuously variable spectral filter from 2.2 to 14 μm; (3) absolute responsivity with a blackbody source and a single bandpass filter from 1.5 to 1.9 μm; (4) absolute responsivity at discrete laser wavelengths of 1.32 and 10.6 μm; and (5) relative spectral responsivity with

a broadband source and monochromator from 0.4 to 2 μm. Methods (2) to (4) provide absolute values through direct comparisons of the VAMWCNT-coated detector to a calibrated transfer standard detector.[16,17] All five measurements provide a picture of the detector's optical absorption efficiency from 400 nm to 14 μm. In every case, the detector evaluation employed a measurement apparatus and procedure that is established at NIST in the category of calibration service.

We elaborate briefly on these five measurements. The reflectance measurement result is absolute and complementary to the absorptance. The reflectance at the detector's surface was referenced to a detector having an identical geometry and known reflectance.[18,19] The absorptance is directly proportional to the relative responsivity from 2.2 to 14 μm.[16] The electrical output of the detector was acquired by means of a current amplifier and lock-in amplifier. The optical signal was modulated with a mechanical chopper referenced to the lock-in amplifier operating at 15 Hz. The detector was thermally stabilized at 22 °C. The infrared responsivity was obtained by two methods using the same blackbody source operating at 1100 °C. In one case, the blackbody source passed through a continuously variable broadband spectral filter. In the other case, the light passed through a single bandpass filter (full width at half-maximum ranging from 1.5 to 1.9 μm). The spectral responsivity over the wavelength range from 0.4 to 2 μm (bandpass less than 10 nm) was determined with a NIST pyroelectric wedge-trap detector that was calibrated using an absolute calorimeter and a second cryogenic radiometer.[20−22]

The absolute responsivity obtained with blackbody sources and spectral filters defines a broad spectral responsivity. This is an adjunct to the absolute responsivity obtained with laser sources, having lower uncertainty. The relative spectral responsivity and the reflectance is reconciled with the absolute responsivity and the uncertainties of each and may be combined to obtain an uncertainty that is typically greater than any individual contribution. In matters of strict calibration at NIST we may state an uncertainty of each datum. In the present work there are several thousand uncertainty values, which we omit in detail. For brevity, we merely state the bounds of uncertainties of the individual measurements. Complete documentation is provided as referenced. The expanded uncertainties have been evaluated with a confidence interval defined as coverage factor, k. The coverage factor of $k = 2$ corresponds to a confidence interval of approximately 95.4% ("two sigma"). The reflectance measurements have an uncertainty ranging from 0.5% at the shortest wavelengths to less than 0.01% at mid-IR range. Measurement results in the range 2.2−14 μm have an expanded uncertainty ranging from approximately 0.4 to 1.9%. Measurement results in the range of 400−1800 nm have an expanded uncertainty that is 1.24% or less. Each datum in Figure 5 represents an average detector signal at each wavelength. Variability more or less than the average

responsivity of 0.375 μA/W is dominated by noise and corresponds with a larger uncertainty that is manifested by a larger Type-A uncertainty contribution (in other words, an uncertainty dominated by a large standard deviation of the datum).

Spatial uniformity measurements were acquired at 1.32 and 10.6 μm by sampling the detector responsivity over a two-dimensional spatial array (99% of the probe-beam energy within circular areas of 400 and 300 μm, respectively) while monitoring and compensating for the amplitude variations of the laser beam. In the central detector area, where the spectral responsivity and reflectance measurements were acquired (approximately 4 mm in diameter), the normalized responsivity shows variations of less than 1%. We have not fully assessed the uncertainty of this measurement but the standard deviation of responsivity at each location is approximately 0.1%. The responsivity variations at 1.32 μm are similar to those at 10.6 μm and indicate the presence of singularities and small coating defects (for example, pinholes near the perimeter that are not apparent by visual inspection). We know that the pyroelectric responsivity is proportional to the detector thickness and we have reported thickness variations as well as polishing and poling defects of the pyroelectric material in the past.[5] The important observation of the spatial uniformity measurement is that, if the reflectance is less than 0.1%, then the coating variations at the 1% level are attributable to the LiTaO$_3$ substrate.

The VAMWCNT samples were imaged using a field-emission scanning electron microscope (FESEM). The VAMWCNT were imaged at an acceleration voltage of 5 kV, using a standard Everhart−Thornley type detector. VAMWCNTs on the witness sample had uniform heights of approximately 16 μm. The VAMWCNTs grown directly on the pyroelectric detector measured 162 μm in height. A series of two images is shown in Figures 2 and 3. Figure 2 shows the witness sample prepared by the method described but on a silicon substrate. Figure 3 is shows the coating on the pyroelectric detector from the same growth run.

The measurement results shown in Figure 4 indicate that the detector reflectance is uniformly less than 0.1% from 400 nm to 4 μm and less than 1% from 4 to 14 μm. These values are slightly higher than the reflectance of the witness sample over the wavelength range from 4 to 14 μm. The detector's responsivity is consistent with the reflectance measurement to the extent that the responsivity is spectrally uniform up to 4 μm. The value of the absolute responsivity is approximately 0.375 μA/W as shown in Figure 5. For comparison, this value is several percent lower than an identical detector that was not exposed to the CVD reactor but having a high-efficiency gold-black coating.[5]

The reduced detector responsivity is attributable to the high-temperature processing of the CVD for two reasons. First, heating the LiTaO$_3$ detector crystal in an oxygen-depleted environment changes the crystals stoichiometry
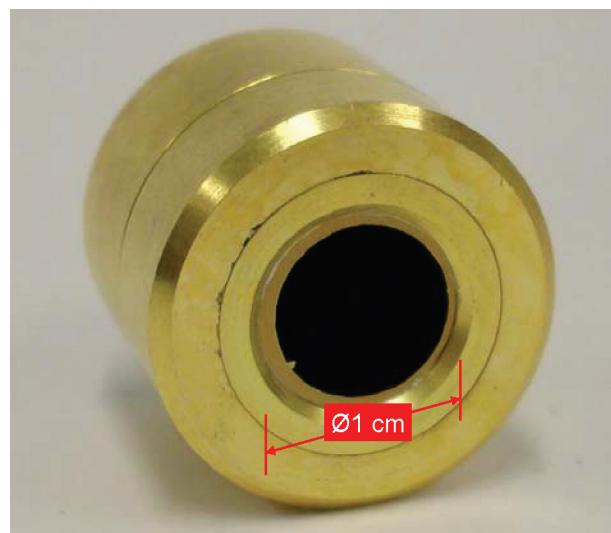
FIGURE 1. The packaged detector. The active area of the detector is approximately 10 mm. The area coated with VAMWCNTs is approximately 8 mm as defined by the deposition of catalyst metal.
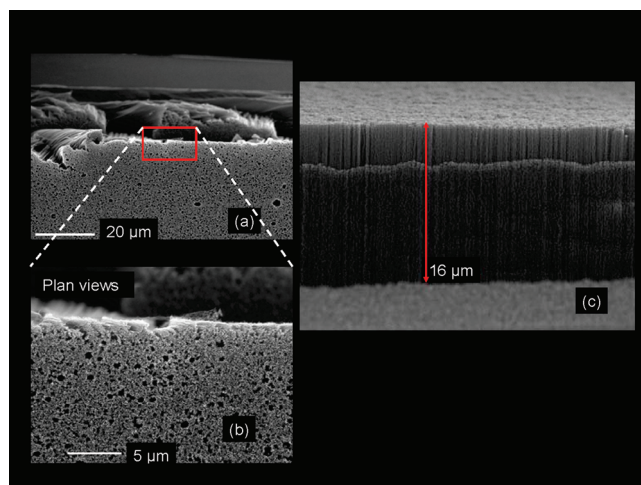
FIGURE 2. SEM images of the witness sample's coating. (a) Viewing the coating along the tube axis, (b) similar view at greater magnification, and (c) a side view of the tube array showing the measured height.

near the surface and increases the surface resistivity and reduces the capacitance.[23,24] Second, the coating deposition was accomplished at a temperature greater than the Curie temperature of LiTaO and we expect the orientation of the spontaneous polarization to be altered.[25] Though we followed the coating deposition with a poling step to restore the spontaneous polarization, some nonuniformity of the crystal structure is still apparent in the spatial response and SEM images such as in Figure 3c. We have experimented with these challenges in earlier work with LiNbO$_3$ pyroelectric detectors coated with MWCNTs. LiNbO$_3$ has a higher Curie temperature (~1100 °C) than LiTaO3 (~665 °C) and so the present result represents significant progress. Surface stoichiometry and repoling bears further investigation and will be the direction of future work. For now, the extremely
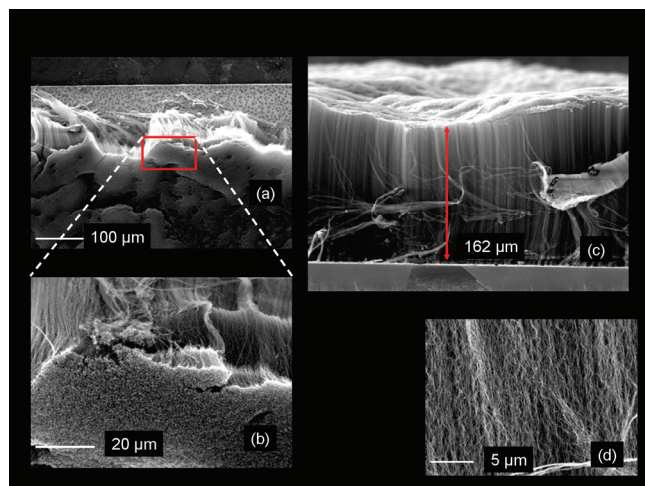
FIGURE 3. SEM images of a detector's coating that is nominally identical to that which was measured for responsivity. (a) Viewing the coating along the tube axis, (b) similar view at greater magnification, (c) a side view of the tube array showing the measured height, and (d) a side view at greater magnification.
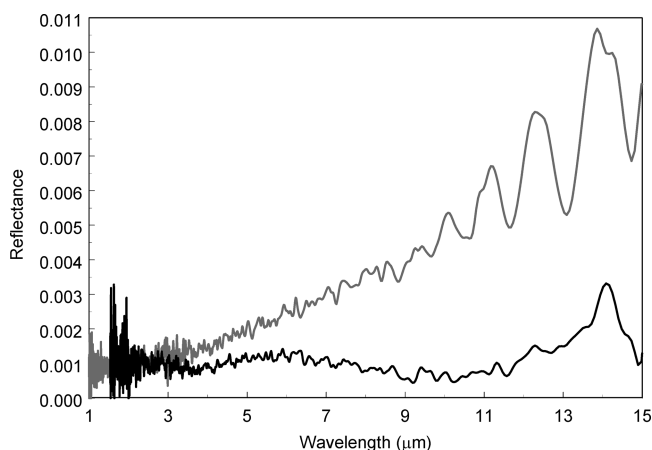

FIGURE 4. Reflectance of (a) VAMWCNT-coated detector, gray line; and (b) VAMWCNT-coated silicon substrate as a witness sample, black line.

FIGURE 5. Absolute responsivity from 0.4 to 14.8 μm of the pyroelectric detector coated with VAMWCNTs. (Solid line) total hemispherical reflectance with FTIR from 1 to 14 μm; (line with open-square data markers) absolute spectral responsivity with a blackbody source and a continuously variable spectral filter from 2.2 to 14 μm; (solid circle) single absolute responsivity with a blackbody source and a single bandpass filter from 1.5 to 1.9 μm; (solid diamonds) absolute responsivity at discrete laser wavelengths of 1.32 and 10.6 μm; (line with open-triangle markers) spectral responsivity with a broadband source and monochromator from 0.4 to 2 μm.

low reflectance on a practical, large-area detector demonstrates a practical and useful application of vertically aligned carbon nanotubes.

We explored several variations with respect to the CVD growth process. Particularly, the processing temperature was varied for different detector samples with and without the repoling operation. Processing temperatures between 650 and 750 °C appeared to degrade the electrical properties of the crystal equally (increased resistance, decreased capacitance). The repoling operation significantly benefits the outcome of the detector performance. The detector responsivity following the nanotube growth was nearly half that of the poled samples. Therefore, assuming we must heat the crystal near the Curie temperature, it does not matter as long as we follow the growth with a poling step. This is a positive result because the optimum growth temperature is clearly above the Curie temperature. This is consistent with
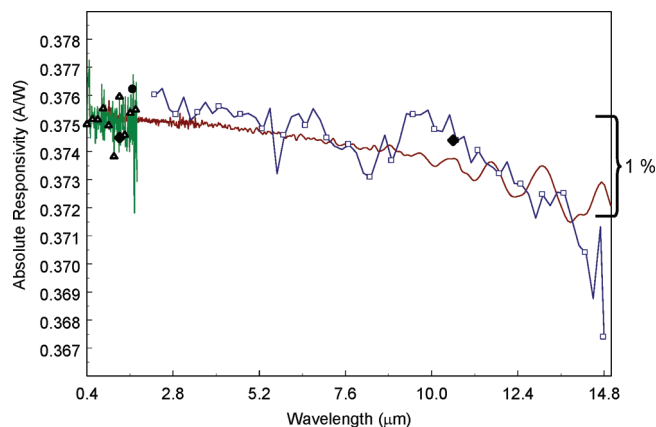
Ci et al.[10] For both the Si witness sample and the pyroelectric detector, the nanotube length increases with CVD growth temperature up to an optimum temperature of approximately 750 °C. Thereafter, increased growth duration corresponds with longer tube length. At growth temperatures below 700 °C it appeared that the tube length on the detector crystal was shorter and less uniform in coverage than on the witness sample, but at 750 °C, the tube length on the detector exceeds that of the witness sample. Future experiments will include an additional step of baking the coated detector in oxygen at low temperature to restore the surface stoichiometry (postgrowth, post poling). The optimal duration and temperature of the final oxygen soak has yet to be explored but the temperature must be sufficiently low to prevent oxidation of the nanotubes.

The difference in reflectance between the detector and the witness is attributable to the coating topology. The low reflectance on the witness sample confirms that lower density is more important than greater length. The detector's reflectance increases and varies periodically at longer wavelengths greater than 4 μm, which is characteristic of optical interference. This is typically a function of the coating thickness (nanotube length). The nanotubes on the detector are apparently dense and less uniform in length compared to the wavelength scale. The nanotubes on the witness are very uniform in height but are characterized by circular gaps (wells) of varying size. The size and distribution of the wells varies with a fractal-like distribution. We know from previous analysis that tube spacing of several diameters will increase the theoretically expected absorption efficiency and uniformity.[8] The reason for the difference in topology between the detector's coating and that of the witness may be attribut-

TABLE 1. Comparison of Reflectance Values of Black Coatings[a]

	wavelength (μm)	approximate reflectance ($\leq$)	witness (W) or detector (D)	reference
carbon paint	10	0.05	W	Betts et al.[26]
platinum black	10	0.03	W	Betts et al.[26]
gold black (on LiTaO3)	10	0.05	D	Lehman et al.[5]
nickel phosphorus (on Cu)	0.6	0.02	W	Kodama et al.[28]
gold black (on Cu)	10	0.01	W	Advena et al.[29]
MWCNTs (mat on LiNbO$_3$)	0.6	0.15	D	Lehman et al.[7]
SWCNTs (mat on LiTaO$_3$)	10	0.75	D	Theocharous et al.[30]
VASWCNTs (on Si)	10	0.01	W	Mizuno et al.[12]
VAMWCNTs (on Si)	0.6	0.0005	W	Yang et al.[11]
VAMWCNTs (on Si)	10	0.001	W	Mizuno et al.[12]
VAMWCNTs (on Si)	0.6	0.001	W	this work
VAMWCNTs (on Si)	10	0.01	W	this work
VAMWCNTs (on LiTaO$_3$)	0.6	0.001	D	this work
VAMWCNTs (on LiTaO$_3$)	10	0.01	D	this work

[a] Note that carbon paint and SWCNT mats have singular nonuniform spectral features having larger reflectance than shown.

able to the detector's electrode metal and the surface properties of LiTaO$_3$. The nature of the metal catalyst formation on top of the detector's metal electrode is important, but we presently do not have enough information to draw conclusions. Nonetheless, this result supports our theoretical work that directs us to templated deposition of the catalyst to optimize the nanotube spacing in the future.[8]

The literature regarding black coatings for optical detectors may be traced to Langley's bolometer and the use of soot to blacken the surface. We find measurements of representative samples, but fewer citations of explicit measurements of reflectance on a detector in the infrared (at 10 um or longer). For example, Betts et al. present a comprehensive summary of infrared reflection properties of black coatings for radiometric detectors with rigorous uncertainties, but the coatings, are on witness samples.[26] Betts et al. indicate that measurements of low reflectance on actual detectors are "not practicable" because of the small size of the detector element, which is typically recessed in some container (package) and in some cases behind a window. In this work, we seize the advantage of our relatively large detector area and the package geometry (shown in Figure 1) to explicitly measure the coating reflectance at the detector's surface. Table 1 includes results from multiple authors for comparison with the present work. The numbers have been approximated from graphical information where necessary. Compared to other materials, VAMWCNTs, as measured on a detector, have nearly one tenth the reflectance in the visible and approximately one-fifth the reflectance at infrared wavelengths. Measurement results from the witness sample present the opportunity for further improvement. Additional information available regarding optical properties of black coatings is available in *The Infrared Handbook*.[27]

Measurement results from the silicon witness sample and the work of other researchers indicate that VAMWCNTs are very attractive from the standpoint of broad, uniform, and efficient optical absorption. We have accomplished a practical application of this science by creating a thermal detector with nearly perfect absorption efficiency in the visible and

near-infrared. Slightly higher reflectance of the pyroelectric-detector's coating in the mid-infrared up to 14 μm leaves room for optimization and qualitative image comparisons with the witness sample indicate properties of the coating that could be improved. For example the thickness of the detector coating could be more uniform in length and less dense. This very black pyroelectric-detector coating provides motivation to seek coatings on other thermal detector platforms and thermal detector cavities. This will benefit a broad range of applications such as accurate measurement of earth and sun irradiance, and absolute calibration of terahertz radiation sources.

REFERENCES AND NOTES

(1) Langley, S. P. The bolometer. *Am. J. Sci.* **1898**, *5*, 241–245.
(2) Becker, W.; Fettig, R.; Gaymann, A.; Ruppel, W. Black gold deposits as absorbers for far infrared radiation. *Phys. Status Solidi B* **1996**, *194*, 241–255.
(3) Advena, D. J.; Bly, V. T.; Cox, J. T. Deposition and characterization of far-infrared absorbing gold black films. *Appl. Opt.* **1993**, *32*, 1136–1144.
(4) Berber, S.; Kwon, Y.; Tománek, D. Unusually High Thermal Conductivity of Carbon Nanotubes. *Phys. Rev. Lett.* **2000**, *84*, 1974–1977.
(5) Lehman, J. H.; Theocharous, E.; Eppeldauer, G.; Pannell, C. Gold-black coatings for freestanding pyroelectric detectors. *Meas. Sci. Technol.* **2003**, *14*, 916–922.
(6) Lehman, J. H.; Engtrakul, C.; Gennett, T.; Dillon, A. C. Single-wall carbon nanotube coating on a pyroelectric detector. *Appl. Opt.* **2005**, *44*, 483–488.
(7) Lehman, J. H.; Hurst, K. E.; Radojevic, A. M.; Dillon, A. C; Osgood, R. M., Jr. Mulitwall carbon nanotube absorber on a thin-film lithium niobate pyroelectric detector. *Opt. Lett.* **2007**, *32*, 772–774.
(8) Theocharous, E.; Deshpande, R.; Dillon, A. C.; Lehman, J. H. Evaluation of a pyroelectric detector with a carbon multiwalled nanotube black coating in the infrared. *Appl. Opt.* **2006**, *45*, 1093–1097.
(9) Ramadurai, K.; Cromer, C. L.; Dillon, A. C.; Mahajan, R. L.; Lehman, J. H. Raman and electron microscopy analysis of carbon nanotubes exposed to high power laser irradiance. *J. Appl. Phys.* **2009**, *105*, No. 093106.
(10) Itkis, M. E.; Borondics, F.; Yu, A; Haddon, R. C. Bolometric Infrared Photoresponse of Suspended Single-Walled Carbon

Nanotube Films. *Science* **2006**, *21*, 413–416, 312.

(11) Yang, Z. P.; Ci, L.; Bur, J. A.; Lin, S.-Y.; Ajayan, P. M. Experimental Observation of an Extremely Dark Material Made By a Low-Density Nanotube Array. *Nano Lett.* **2008**, *8*, 446–451.

(12) Mizuno, K.; Ishii, J.; Kishida, H.; Hayamizu, Y.; Yasuda, S.; Futaba, D. N.; Yumura, M.; Hata, K. A black body absorber from vertically aligned single-walled carbon nanotubes. *Proc. Natl. Acad. Sci. U.S.A.* **2009**, *106*, 16044–16047.

(13) Lijie, Ci; Vajtai, Robert; Ajayan, P. M. Vertically Aligned Large-Diameter Double-Walled Carbon Nanotube Arrays Having Ultralow Density. *J. Phys. Chem. C* **2007**, *111*, 9077–9080.

(14) Hanssen, L. M.; Kaplan, S. G. Infrared diffuse reflectance instrumentation and standards at NIST. *Anal. Chim. Acta* **1998**, *380*, 289–302.

(15) Hanssen, L. M.; Snail, K. A. Integrating Spheres for Mid- and Near Infrared Reflection Spectroscopy. In *Handbook of Vibrational Spectroscopy*; Chalmers, J. M., Griffiths, P. R., Eds.; John Wiley & Sons, Ltd: New York, 2002; Vol. 2, pp 1175−1192.

(16) Lehman, J.; Eppeldauer, G.; Aust, J. A.; Racz, M. Domain Engineered pyroelectric radiometer. *Appl. Opt.* **1999**, *38*, 7047–7055.

(17) Eppeldauer, G. P.; Zeng, J.; Yoon, H. W.; Wilthan, B.; Larason, T. C.; Hanssen, L. M. Extension of the NIST spectral responsivity scale to the infrared using improved-NEP pyroelectric detectors. *Metrologia* **2009**, *46*, S155–S159.

(18) Zeng, J.; Hanssen, L. M. Calibration of the spectral radiant power responsivity of windowed pyroelectric radiometers from 785 nm to 14 μm. *Proc. of SPIE* **2008**, *7082*, 70820Y.

(19) Lykke, K. R.; Shaw, P. S.; Hanssen, L. M.; Eppeldauer, G. P. Development of a monochromatic, uniform source facility for calibration of radiance and irradiance detectors from 0.2 μm to 12 μm. *Metrologia* **1998**, *35*, 479–484.

(20) Lehman, J. H. Calibration Service for Spectral Responsivity of Laser and Optical-Fiber Power Meters at Wavelengths Between 0.4 μm and 1.8 μm. *Natl. Inst. Stand. Technol. Spec. Publ.* **1999**, *250−53*, 1–39.

(21) Lehman, J. H. Pyroelectric trap detector for spectral responsivity measurements. *Appl. Opt.* **1997**, *36*, 9117–9118.

(22) Livigni, D. High-Accuracy Laser Power and Energy Meter Calibration Service. *Natl. Inst. Stand. Technol. Spec. Publ.* **2003**, *250−62*, 1−39, 1−144.

(23) Houe, M.; Townsend, P. D. An introduction to methods of periodic poling for second-harmonic generation. *J. Phys. D: Appl. Phys.* **1995**, *28*, 1747–1763.

(24) Young, S. L.; Kao, M. C.; Chen, H. Z. Optical Properties of LiTaO3 Thin Films crystallized by RTA processes. *J. Electroceram.* **2006**, *17*, 799–803.

(25) Lehman, J. H.; Deshpande, R.; Rice, P.; To, B.; Dillon, A. C. Carbon multi-walled nanotubes grown by HWCVD on a pyroelectric detector. *Infrared Phys. Technol.* **2005**, *47*, 246–250.

(26) Betts, D. B.; Clarke, F. J. J.; Cox, L. J.; Larkin, J. A. Infrared reflection properties of five types of black coating for radiometric detectors. *J. Phys. E: Sci. Instrum.* **1985**, *18*, 689–696.

(27) Wolfe, W. L. Zissis, G. J. *The infrared handbook*; Environmental Research Institute of Michigan: Ann Arbor, MI, 1989; pp 7.78−7.80.

(28) Kodama, S.; Horiuchi, M.; Kunii, T.; Kuroda, K. Ultra-Black Nickel-Phosphorous Alloy Optical Absorber. *IEEE Trans. Instrum. Meas.* **1990**, *39*, 230–232.

(29) Advena, D. J.; Bly, V. T.; Cox, J. T. Deposition and characterization of far-infrared absorbing gold black films. *Appl. Opt.* **1993**, *32*, 1136–1144.

(30) Theocharous, E.; Engtrakul, C.; Dillon, A. C.; Lehman, J. Infrared responsivity of a pyroelectric detector with a single-wall carbon nanotube coating. *Appl. Opt.* **2008**, *47* (22), 3999–4003.